

MICHIGAN STATE UNIVERSITY

CYCLOTRON LABORATORY

FORM FACTORS IN THE INTERACTING BOSON MODEL

O. SCHOLTEN

To be published in the Proceedings of the "International Workshop
on Interacting Boson-Boson and Boson-Fermion Systems" held at
Gull Lake, MI, May 28-30, 1984



SEPTEMBER 1984

MSUCL-480

FORM FACTORS IN THE INTERACTING BOSON MODEL

O. Scholten

Cyclotron Laboratory and Department of Physics-Astronomy
Michigan State University, East Lansing, MI 48824

ABSTRACT

Microscopic calculations of form factors and transition densities in the framework of the IBA model are presented. As an example E2 transition densities are calculated for ^{110}Pd , and special attention is paid to the problem of core polarization. Also magnetic transitions have recently received much attention since they are related to states in the IBA model that are not fully symmetric in the neutron and proton degrees of freedom. Calculations the M1 form factor are compared with experiment and a prediction is given for the M3 form factors.

1. INTRODUCTION

The interest in the calculation of transition densities and form factors for medium heavy nuclei is growing now high resolution electron scattering experiments can be performed. In the contributions of de Jager et al.¹⁾ and Goutte et al.²⁾ to this conference several examples of such experiments are shown.

In the IBA model framework, form factors have been calculated using a phenomenological approach.³⁾ In this talk we will focus on the calculation of form factors in IBA starting from a microscopic model. To show the flexibility and the predictive power of IBA, we will first give a short review of the phenomenology for E2 transition densities. These are calculated in the IBA model by generalizing the E2 transition operator to

$$\hat{\rho}_{\text{E2}}^{\text{E2}}(r) = \alpha(r) (s_{\text{d}}^{\dagger} + d_{\text{s}}^{\dagger})^{(2)} + \beta(r) (d_{\text{d}}^{\dagger})^{(2)} \quad (1.1)$$

The transition density for a specific $0 \rightarrow 2$ transition is now given by

$$\rho_{0 \rightarrow 2_n}(r) = \alpha(r) A + \beta(r) B \quad , \quad (1.2)$$

where

$$A = \langle 0 || s^\dagger \bar{d} + d^\dagger s || 2_n \rangle / \sqrt{5} , \quad (1.3)$$

and

$$B = \langle 0 || (d^\dagger \bar{d})^{(2)} || 2_n \rangle / \sqrt{5} \quad (1.4)$$

are coefficients which are readily calculable in the IBA model and are state dependent. The functions α and β are only dependent upon the microscopic structure of the bosons and are taken to be the same for all levels in a given nucleus. In a phenomenological analysis of transition densities therefore the two functions $\alpha(r)$ and $\beta(r)$ can be obtained from unfolding two measured transition densities and can subsequently be used to predict the other transition densities.

In this contribution the emphasis is put on the microscopic calculation of transition densities. The focus will be put on the general features of the calculation. The approach taken here to calculate the structure functions $\alpha(r)$ and $\beta(r)$ is in philosophy similar to what has been done in the calculation of the parameters of the IBA Hamiltonian for spherical nuclei⁴⁾; form factors are calculated for lowest seniority states in the shell model and subsequently equated to the corresponding form factors in the IBA model. In the shell model calculation we used a truncation⁵⁾ on generalized seniority⁶⁾ as outlined in section 2. As a first example, the calculation of E2 transition densities for ^{110}Pd is discussed in section 3. Special attention is paid to the problem of core polarization. Magnetic transitions are in this respect simpler, and as an example a calculation is presented for the recently measured M1 form factor in ^{156}Gd ⁷⁾ in section 4. Also a prediction is given for the M3 form factor in deformed nuclei.

2. THE GENERALIZED SENIORITY SCHEME

In this section an outline is given of the generalized seniority (g.s.) model, which is used in the calculation of transition densities and form factors. A more detailed account of the model can be found in ref. 5.

The g.s. scheme is in spirit similar to the seniority scheme, as introduced by Talmi.⁶⁾ The S-pair creation and annihilation operators,

$$S_+ = \sum_j \alpha_j \frac{1}{2} \sqrt{2j+1} (a_j^\dagger a_j^\dagger)^{(0)} \quad (2.1)$$

and

$$S_- = S_+^\dagger$$

are closely related to the s-boson in the IBA model. Unlike the normal seniority scheme, the operators (2.1) cannot be completed with a third to form the generators of an SU(2) Lie algebra. This prevents the introduction of rigorous quantum numbers, but the states can still be labelled with an approximate g.s. quantum number w , which, in essence, measures the number of particles in the state that cannot be grouped together in an S-pair state, as defined by eq. (2.1). A $w=0$ state is unique (given the coefficients α_j) and has $J^\pi=0^+$. In a multi-j shell space there exist in general several $w=2$ states with the same J^π value. Due to the absence of an underlying group symmetry also the calculation of matrix elements is more involved than in the normal seniority scheme, but can still be done exactly.⁸⁾

For semi closed shell nuclei the g.s. scheme offers a powerful truncation scheme for shell model calculations. To illustrate this, the results of different calculations for ^{144}Sm are compared in Fig. 1. In the g.s. calculation exactly the same Hamiltonian is used as in the shell model calculation,⁹⁾ but the model space is smaller by more than two orders of magnitude. The coefficients α_j (see eq. (2.1)) are chosen, using an iterative procedure, such that there is no direct mixing between the $w=0$ and the $w=2$ states.⁵⁾ The $|n=2N, w=0, J=0\rangle \equiv |S^N\rangle$ ground state obtained from such a calculation is identified with the $|s^N\rangle$ state in the IBA model and the $|n=2N, w=2, J=2\rangle \equiv |S^{N-1}D\rangle$ state with the $|s^{N-1}d\rangle$ state.

In the case that both neutrons and protons are active the approach has to be refined. The n-p force strongly mixes seniority since it is dominated by a quadrupole-quadrupole (Q.Q) interaction. To be able to take this into account in lowest order, the $J=0$ model space, for example, is extended by including states of the kind

$$S_{\pi}^{(N_{\pi}-1)} S_{\nu}^{(N_{\nu}-1)} (D_{\pi} D_{\nu})^{(0)}, \text{ and } S_{\pi}^{(N_{\pi}-1)} S_{\nu}^{(N_{\nu}-1)} (G_{\pi} G_{\nu})^{(0)}, \text{ where the}$$

MSU-83-236

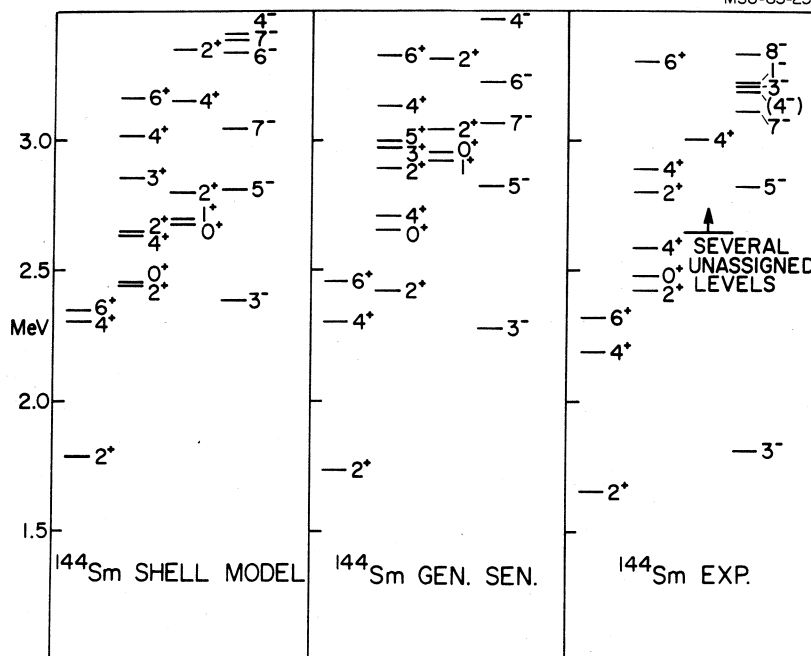


Fig. 1 - The spectrum of ^{144}Sm calculated in the generalized seniority scheme is compared with the shell model calculation of ref. 9 and the experimental spectrum.

G-pair state is defined as the lowest $w=2, J=4$ state. In the neutron-proton interaction both the quadrupole and hexadecupole components are considered,

$$V_{\pi\nu} = -\kappa_2 r_0^{-4} (r_{\pi}^2 Y_{\pi}^{(2)})(r_{\nu}^2 Y_{\nu}^{(2)}) - \kappa_4 r_0^{-8} (r_{\pi}^4 Y_{\pi}^{(4)})(r_{\nu}^4 Y_{\nu}^{(4)}), \quad (2.2)$$

where

$$r_0^{-2} = (m\omega_0/\hbar) \quad .$$

From the analysis of the empirical matrix elements of the n-p interaction by Schiffer¹⁰⁾ it follows that the hexadecupole component is roughly half that of the quadrupole.

3. E2 TRANSITION DENSITIES

Following the philosophy of the OAI⁴⁾ approach, the densities $\alpha(r)$ and $\beta(r)$, which enter in the description of E2 densities in the IBA

model, are determined from the quadrupole transition densities in a shell-model calculation for lowest seniority states,

$$\alpha(r) = \rho_F^{E2}(S^N \rightarrow S^{N-1}D) / \sqrt{5N} \quad (3.1)$$

and,

$$\beta(r) = \rho_F^{E2}(S^{N-1}D \rightarrow S^{N-1}D) / \sqrt{5} \quad (3.2)$$

where the shell-model S and D pair states are defined as outlined in the previous section. We will discuss here the approach for $\alpha(r)$.

Matrix elements (m.e.) between multi-particle model states of a one-body tensor operator are conveniently expressed¹¹⁾ as a sum over m.e. of the one-body density matrix (OBDM) and the corresponding m.e. of the single-nucleon transition density (SNTD),

$$\rho_F^{E2}(S^N \rightarrow S^{N-1}D) = \sum_{j,j'} \text{OBDM}(2,j,j') \text{SNTD}(E2,j,j',r) \quad (3.3)$$

where

$$\text{OBDM}(\lambda,j,j') = \langle S^N || (a^\dagger_{\tilde{a}})^{(\lambda)} || S^{N-1}D \rangle / \sqrt{(2\lambda+1)} \quad (3.4)$$

and

$$\text{SNTD}(E\lambda,j,j',r) = R(j,r) R(j',r) \langle j || e Y^{(\lambda)} || j' \rangle \quad (3.5)$$

where e is the nucleon charge and $\lambda=2$ for E2 transitions. The j, j' summation extends over all valence orbits. The radial wave functions $R(j,r)$ are calculated using a Woods-Saxon single particle potential.

We will present here the results of calculations for ^{110}Pd for which the densities $\alpha(r)$ and $\beta(r)$ shown in Fig. 2 have been determined from an experimental analysis.¹⁾ In a first calculation only the $0f_{7/2}$, $1p_{3/2}$, $1p_{1/2}$, $0g_{7/2}$ orbits were taken into account for the protons and the 50-82 major shell for neutrons. The interaction between like particles is taken to be a surface delta interaction with an enhanced quadrupole component (SDIQ).⁵⁾ The force parameters were chosen as to reproduce the energies of the 2_1^+ and 4_1^+ levels of semi closed shell nuclei, $A=0.2$ MeV, $F_2=1.5$ for protons and $A=0.18$ MeV, $F_2=1.9$ for neutrons. The single particle energies used are given in Table 1. The strength of the neutron-proton interaction (2.2) is taken equal to $\kappa_2=.08$ MeV, and $\kappa_4=.0016$ MeV. This is comparable to the value taken in

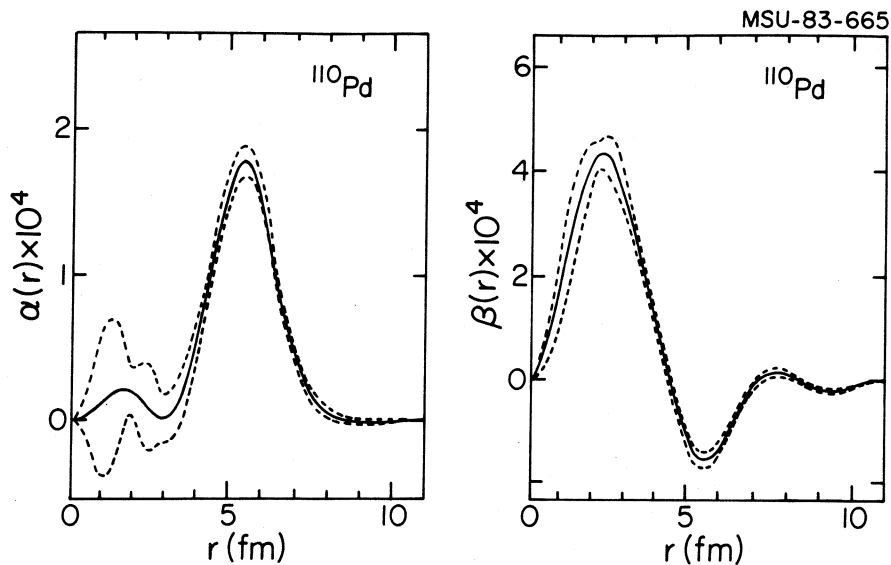


Fig. 2 - Transition densities $\alpha(r)$ and $\beta(r)$ as extracted by de Jager et al.¹⁾ from electron scattering data on ^{110}Pd .

the analysis of the Sm isotopes,⁵⁾ and gives the correct value for the boson-boson quadrupole force. The thus determined S- and D-pair wave

Table 1 - Relative single particle energies (in MeV) as used in the calculations for ^{110}Pd .

Neutrons		Protons	
$0g_{7/2}$	0.5	$0f_{5/2}$	-1.6
$1d_{5/2}$	0.0	$1p_{3/2}$	-1.4
$1d_{3/2}$	2.5	$1p_{1/2}$	-1.04
$2s_{1/2}$	2.0	$0g_{9/2}$	0.0
$0h_{11/2}$	2.9	$0g_{7/2}$	5.9
		$1d_{5/2}$	6.9

functions are used to calculate the densities $\alpha(r)$ and $\beta(r)$, shown in Fig. 3, where they are compared with the densities extracted from the experimental analysis. It can be seen that the major features are being reproduced, $\alpha(r)$ is peaked at the surface of the nucleus while $\beta(r)$ is changing sign. There are also some marked discrepancies. The calculated $\alpha(r)$ has an additional peak in the interior for which there is

ample evidence in the experiment, while the value at the surface is only half the experimental value. In $\beta(r)$ the position of the outermost extreme and zero crossing point are located too much at the inside. As is well known from shell-model calculations, some of these

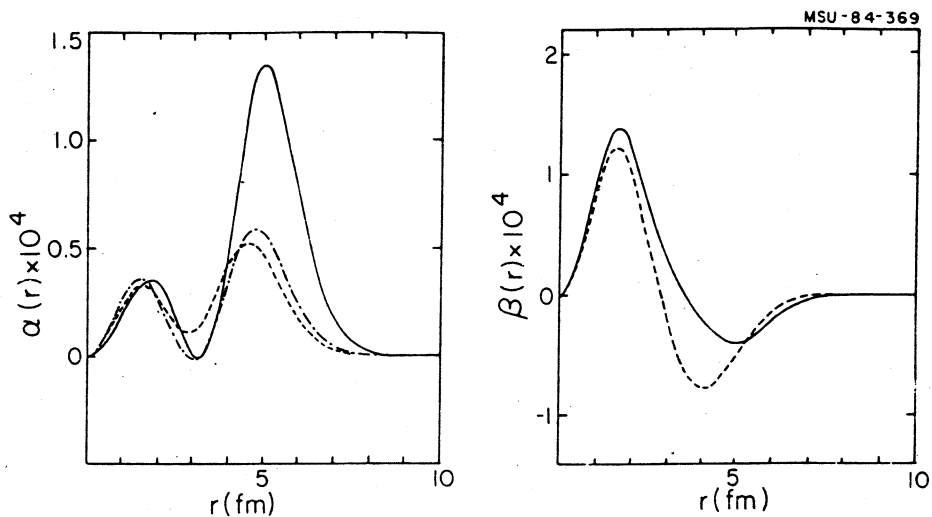


Fig. 3 - The calculated transition densities $\alpha(r)$ and $\beta(r)$, the dashed curves represent the results of the calculation in the small basis, the dash-dotted curves those in the larger basis, and for the drawn curves a Tassie density has been added with an effective charge of 0.7.

effects are a result of the use of a limited model space, i.e. core polarization.

In a recent¹²⁾ investigation of transition densities in the s-d shell, two methods have been used to take into account core polarization effects, both giving similar agreement with the data, i) by multiplying the valence transition density by a constant factor or, ii) by adding a Tassie¹³⁾ density to the calculated transition density. From Figs. 2 and 3 it is clear that in heavy nuclei the first approach will not give satisfactory results. Also the second approach is unsatisfactory, a Tassie density (the derivative of the ground state density) is namely strongly peaked at the surface. The position of the sign change in $\beta(r)$ will not be affected by this. For this reason we investigated the effects of the size of the model space explicitly by repeating the calculations using larger space for the protons by including the $1d_{5/2}$ and $0g_{7/2}$ proton orbits which lie above the Z=50 shell gap. These orbits are of principal interest since the quadrupole operator has nonvanishing matrix elements between these and the most active valence orbit, the $0g_{7/2}$. The used s.p. energies are given in Table 1. The strengths of the interactions are taken the same as

before. It has been checked that the results obtained for semi-closed shell nuclei remained essentially unchanged. The new $\alpha(r)$ and $\beta(r)$ are given in Fig. 3. The improvement over the calculations done in the smaller basis are mostly in $\beta(r)$.

Since in Pd the proton bosons are hole-like, questions may arise about the proper counting of the number of bosons in the extended model basis. If the number of holes are counted in the larger model space, one would have to introduce nine proton bosons instead of two. The effective number of bosons, calculated using the procedure described in ref. 14, remains however essentially unchanged by the extension of the model basis.

The extension of the model space influences $\alpha(r)$ and $\beta(r)$ mainly through the effect of the neutron-proton quadrupole interaction. This implies that it is especially important for the calculation of quadrupole form factors to include the effect of the n-p quadrupole force on the structure of the S- and D-fermion pair states. In the present approach this has been done in a first-order approximation, which, for close to spherical nuclei, is probably sufficient. For deformed nuclei more care should be taken into account, our procedure would probably underestimate the effects of model space truncation.

In the larger basis only part of the effects of core polarization are recovered. To increase the model space even further is impractical and we therefore assume that the additional core polarization can be taken into account by a Tassie density, which in Fig. 3 is included with an effective charge of 0.7. For states that are symmetric in the neutron and proton degrees of freedom the core polarization adds up constructively at the surface of the nucleus. For mixed symmetry states, the core polarization adds destructively on the surface, which might give an opportunity to distinguish symmetric and antisymmetric states in electron scattering.

In a single j-shell model one would expect the same functional dependence on r for both α and β . To understand the differences, a more detailed investigation of the coherence of the s.p. contributions to $\alpha(r)$ and $\beta(r)$ has to be made. Since in calculating the B(E2) value the densities are weighted by r^2 , the most collective B(E2) value is obtained if in $\alpha(r)$ all amplitudes add up constructively in the surface

region of the nucleus. In the calculation of $\beta(r)$ the situation is different. From seniority consideration one expects little collectivity, for a half-filled shell the quadrupole moment of a $\nu=2$ state, which corresponds to the integrated value of $r^2\beta(r)$, equals zero. In the case of the Pd isotopes, the negative parity proton s.p. levels lie below the fermi energy and give an opposite contribution to $\beta(r)$ than the positive parity levels lying above the fermi level. Because of the difference in the radial wave functions, this destructive interference in the quadrupole moment results in a density that has a positive and an almost-as-strong negative lobe. In a geometric model, $\alpha(r)$ is related to the first, and $\beta(r)$ to a second derivative of the ground-state density, which offers an alternative explanation.

4. MAGNETIC FORM FACTORS

Recently much attention is focussing on magnetic transitions. It has been suggested by various authors¹⁵⁻²⁰⁾ that if in collective models a distinction is made between neutron and proton degrees of freedom a low-lying collective 1^+ state is present. In particular in the deformed region, where this state is the bandhead of a $K^\pi=1^+$ band, it is connected to the ground state by a relatively large M1 matrix element. The geometric interpretation of such a $K^\pi=1^+$ mode is that of a small amplitude oscillation in terms of the angle between the two symmetry axes of an axially symmetric deformed neutron and proton distribution.^{15,17)}

In the neutron-proton IBA model, where this state is based on a configuration that is not fully symmetric, hereafter referred to as anti-symmetric, in the n-p degrees of freedom,²¹⁾ a simple sum rule for the expected M1 strength was derived,^{17,18)} which stimulated electron scattering experiments⁷⁾ to search for this strength. At present there exist indications for appreciable M1 strength ($1-2 \mu_N^2$) at $E_x \approx 3$ MeV in several rare-earth nuclei.^{22,23)} Since M1 transitions are predominantly isovector in character, it is crucial to distinguish explicitly the neutron and proton degrees of freedom in the calculation. In the IBA-2 model the M1 transition operator is given by

$$F^{M1}(q) = g_v(q) (d_v^\dagger \tilde{d}_v)^{(1)} + g_\pi(q) (d_\pi^\dagger \tilde{d}_\pi)^{(1)} \quad , \quad (4.1)$$

where q is the momentum transfer. In the case of magnetic transitions it is to be preferred to work directly with the form factors since both spin and convection currents can give a contribution. To calculate the M1 form factors a similar approach will be followed as in the calculation of E2 transition densities, however instead of using a single-nucleon transition density, we introduce a single-nucleon form factor (SNFF),

$$\begin{aligned} \text{SNFF}(M1, j, j', q) = & \int d^3r R(j, r) R(j', r) j_1(qr) Y_{11}(\hat{r}) \\ & \times \langle j || J^{M1} || j' \rangle \end{aligned} \quad (4.2)$$

where J^{M1} is the M1 current operator.²⁴⁾ The definition of OBDM remains unchanged.

As a typical example of the M1 form factor in the IBA model we present here the results of a calculation for ¹⁵⁶Gd. The M1 form factor has been measured for this nucleus and a direct comparison between theory and experiment is thus possible. In the microscopic calculation we used the g.s. model. The interaction used is a SDIQ with $A=0.2$ MeV, and $F_2=1.5$ for protons and $A=0.13$ MeV, and $F_2=1.4$ for neutrons, as to

Table 2 - Relative single particle energies (in MeV) as used in the calculations for the rare earth nuclei.

Neutrons		Protons	
1f _{7/2}	0.0	0g _{7/2}	0.0
0h _{9/2}	0.78	1d _{5/2}	0.98
2p _{3/2}	1.49	1d _{3/2}	2.61
0i _{1/2, 3/2}	1.06	2s _{1/2}	2.92
1f _{5/2}	2.93	0h _{11/2}	2.44
2p _{1/2}	2.26		

reproduce the energies of the 2⁺ and 4⁺ levels in semi-closed shell nuclei. The s.p. energies used are given in Table 2. In the calculations the n-p force was not taken into account as core polarization does not play an important role for magnetic transitions since in a multipole expansion of the n-p force the magnetic multipoles play a minor role.

In Fig. 4 the calculated collective M1 form factor is

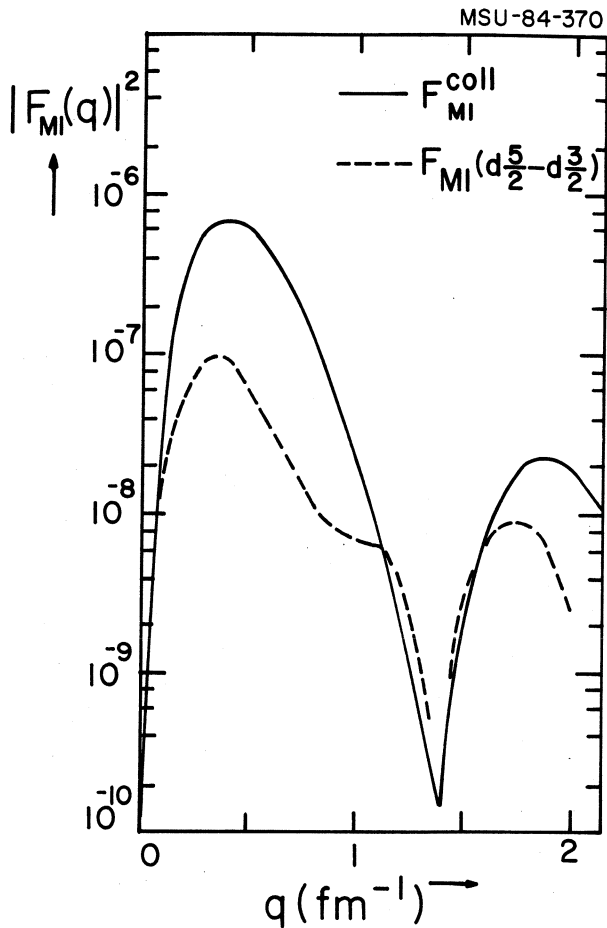


Fig. 4 - A typical collective and single particle M1 form factor. The spin g-factor is quenched by 70%.

this K=1 band. One particularly interesting mode to study is magnetic octupole transitions. In the IBA-2 approach the M3 operator is the lowest order boson operator of rank 3,

$$T_{\mu}^B(M3, q) = \sqrt{\frac{35}{8\pi}} \left\{ \Omega_{\pi}(q) (d_{\pi}^{\dagger} \tilde{d}_{\pi})_{\mu}^{(3)} + \Omega_{\nu}(q) (d_{\nu}^{\dagger} \tilde{d}_{\nu})_{\mu}^{(3)} \right\} \quad (4.3)$$

where Ω_{ρ} ($\rho = \nu, \pi$) are the magnetic octupole moments of the neutron and proton d-boson.

The calculation of the M3 form factor proceeds in the same way as for the M1 transitions. The expression for the single-nucleon form factor now reads²⁴⁾

compared with that of a typical 2 q.p. proton transition. The big difference between the two arises from the fact that in the collective M1 the spin current hardly contributes and thus arises purely from the proton convection current. On the average there are as many spin up as spin down levels contributing to the collective M1 which is not the case for a 2 q.p. transition. The collective form factor is compared with experiment in Fig. 5. The calculated M1 strength agrees well with the measured value of $1.3 \mu_N^2$.

These developments suggest a further investigation of the higher angular momentum members of

$$\text{SNFF}(M3, j, j', q) = \sqrt{\frac{8\pi}{5}} \int d^3r R(j, r) R(j', r) j_3(qr) \times Y_{33}(\hat{r}) \langle j || J^{M3} || j' \rangle \quad (4.4)$$

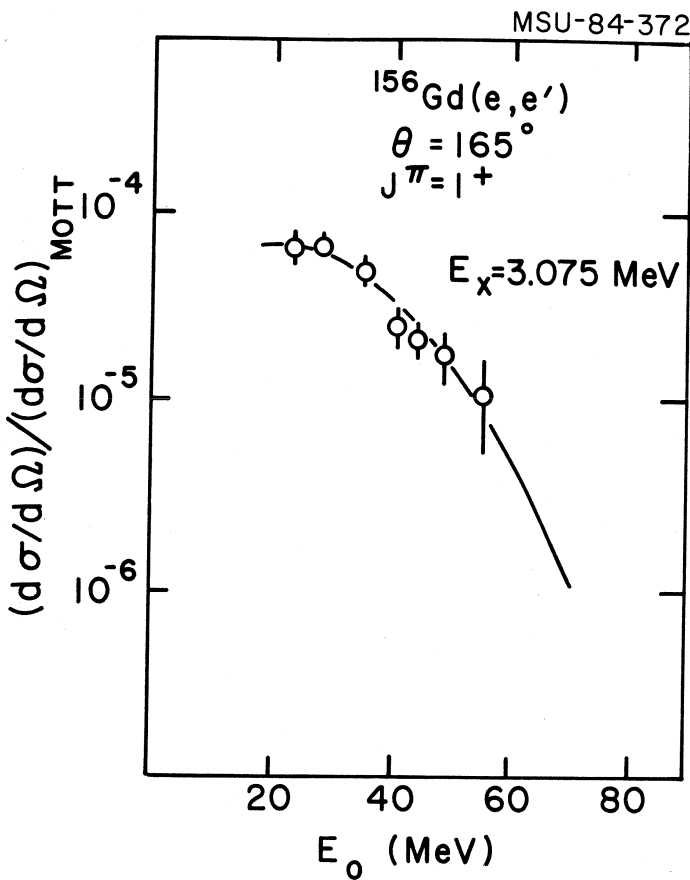


Fig. 5 - Comparison of the calculated collective M1 form factor with experiment.⁷⁾

the form factor for Gd at $q=1.5 \text{ fm}^{-1}$ is the result of an accidental complete cancellation of the spin and orbital contribution at this momentum transfer. It depends sensitively on the precise values of the parameters, and for example a slight change in s.p. energies can make this minimum disappear. One might therefore expect that, by including the effect of the n-p interaction, which leads to increased collectivity of the S and D pairs in the microscopic calculation, the variations are washed out.

To obtain a measure of the strength of the M3 transition we calculated the $B(M3)$ values for a realistic case. In near spherical

In the microscopic calculations the neutrons and protons have been considered separately, thus ignoring the effects of the neutron-proton interaction. For the neutron and proton spin magnetic moments a quenching factor of 0.7 is used. In Fig. 6 the results of the calculation are presented for $\Omega_{\pi}(q)$ in the Nd, Sm, and the Gd isotopes. The form factor shows a strong dependence on nucleon number, which is particularly strong in this mass region due to the Z=64 sub-shell closure. The minimum in

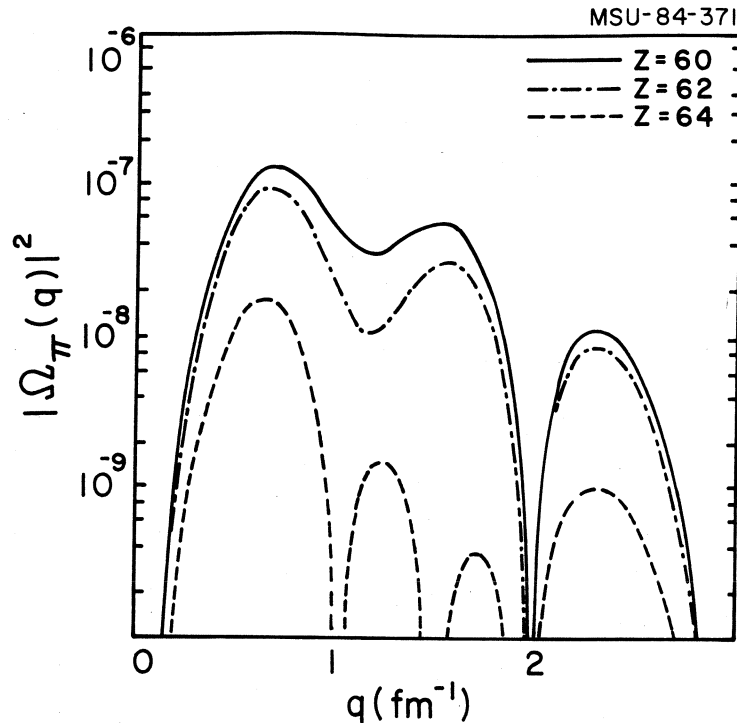


Fig. 6 - Some calculated octupole form factors for the proton d-boson. The spin g-factor is quenched by 70%.

nuclei, the SU(5) limit of the IBA applies; and, due to the d-boson conserving character of the M3 operator, all M3 transitions leading to the ground state vanish. In the SU(3), the axially symmetric rotor, limit the picture is more complex. The operator (1) connects the ground state, $(\lambda, \mu) = (2N, 0), L=0$ with $L^\pi = 3^+$ states in the gamma-band [i.e. the symmetric SU(3) representation $(\lambda, \mu) = (2N-4, 2)$], in the $(\lambda, \mu) = (2N-2, 1), K=1$ band, and in the anti-symmetric $(\lambda, \mu) = (2N-4, 2), K=2$ band. We therefore choose the deformed nucleus ^{154}Sm as our bench mark case.

The numerical calculations were performed using the standard IBA-2 Hamiltonian, using the parameters of ref. 25. Only the strength of the Majorana force has been readjusted to $\xi_1 = \xi_2 = \xi_3 = 0.15$ MeV such that the 1^+ state lies at about 3 MeV, where it has been observed⁷⁾ in ^{156}Gd . In Table 3 the levels are labelled by their K values and the symmetry character (totally symmetric (s) or antisymmetric (a)). Note, however, that the IBA-2 Hamiltonian will in general lead to some mixing of both

Table 3. Calculated excitation energies (in MeV) and $B(M3, 0 \rightarrow 3^+)$ values for the first four collective 3^+ states in ^{154}Sm in units of $\mu_N^2 b^2$.

state	band	E_x	$B(M3^+)$
3_1^+	2_1^s	1.51	0.23
3_2^+	2_2^s	2.46	0.001
3_3^+	1_1^a	2.99	0.56
3_4^+	2_1^a	3.26	0.31

K and symmetry character and therefore the labels refer only to the dominant components in the wave function. As expected three 3^+ levels are excited in the SU(3) limit. The single particle value for a M3 transition is $0.13 \mu_N^2 b^2$ while the typical strength of a transition to the first 2 q.p. 3^+ state, as calculated

in the generalized seniority model,¹²⁾ is only of the order of $0.03 \mu_N^2 b^2$. Comparing this with the values given in Table 3 it can be seen

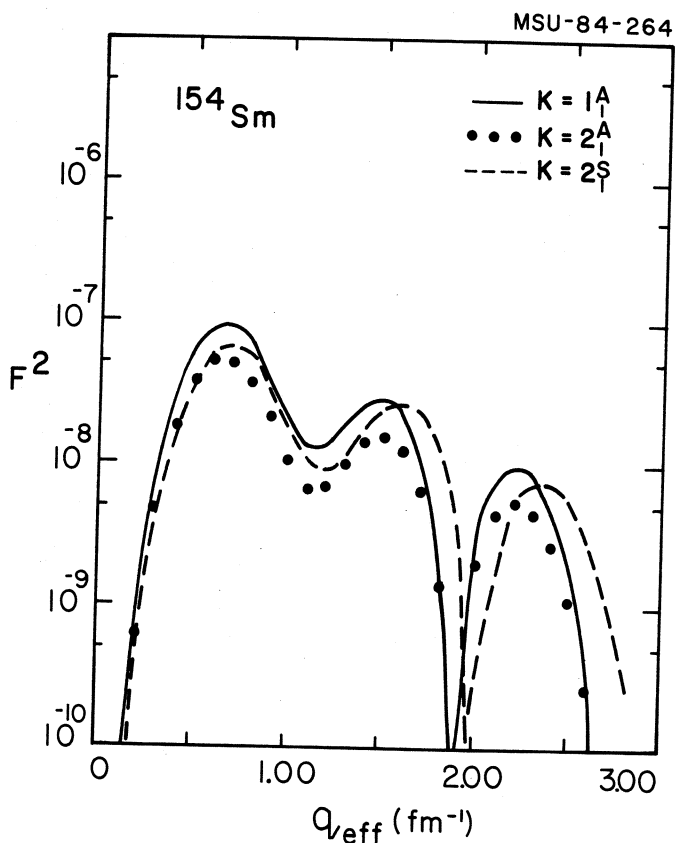


Fig. 7 -The calculated form factors for the three strongest excited 3^+ states in the spectrum of ^{154}Sm .

that the values given in the table are an order of magnitude larger, clearly indicating collectivity.

In Fig. 7 the form factors are given for the three strongest $0 \rightarrow 3^+$ transitions in ^{154}Sm . For smaller values of Z the minimum near $q_{\text{eff}} = 1 \text{ fm}^{-1}$ quickly disappears.

5. CONCLUSIONS

The results of microscopic calculations of transition densities and form factors in the framework of the IBA model have been presented. The

results for E2 densities showed a considerable sensitivity to the size of the model space and core polarization effects are very important. This makes E2 densities a sensitive test of the intrinsic structure of the bosons. Core polarization has been included by adding a Tassie density to the valence contribution, but in a more extensive treatment the method described in ref. 26 is preferable. The calculated M1 form factor is in good agreement with the data. It is interesting to investigate experimentally predicted collective M3 transitions.

REFERENCES

1. C. W. de Jager, Invited paper, International Workshop on Interacting Boson-Boson and Boson-Fermion Systems, Gull Lake, Michigan 1984.
2. D. Goutte, J. M. Bazantay, W. Boeglin, J. M. Cavedon, B. Frois, M. Huet, P. Leconte, X. H. Phan, S. K. Platchkov and I. Sick, Invited paper, International Workshop on Interacting Boson-Boson and Boson-Fermion Systems, Gull Lake, Michigan 1984.
3. A.E.L. Dieperink, F. Iachello, A. Rinat, C. Creswell, Phys. Lett. 76B (1978) 135.
A.E.L. Dieperink, Nucl. Phys. A358 (1981) 189c.
4. T. Otsuka, A. Arima, and F. Iachello, Nucl. Phys. A309 (1978) 1.
5. O. Scholten, Phys. Rev. C28 (1983) 1783.
6. I. Talmi, Nucl. Phys. A172 (1971) 1.
7. D. Bohle, A. Richter, W. Steffen, A.E.L. Dieperink, N. Lo Iudice, F. Palumbo, and O. Scholten, Phys. Lett. 137B (1984) 27.
8. O. Scholten and S. Pittel, Phys. Lett. 120B (1983) 9.
9. H. Kruse and B.H. Wildenthal, Bull. Am. Phys. Soc. 27 (1982) 533, 27 (1982) 725.
10. J.P. Schiffer and W.W. True, Rev. Mod. Phys. 49 (1976) 191.
11. B.A. Brown, Computer Program DENS.
12. B.A. Brown, R. Radhi and B.H. Wildenthal, Phys. Rep. 101 (1983) 313.
13. L.J. Tassie and F.C. Barker, Phys. Rev. 111 (1958) 940.
14. O. Scholten, Phys. Lett. 127b (1983) 144.
15. N. Lo Iudice and F. Palumbo, Phys. Rev. Lett. 41 (1978) 1532;

- ibid, Nucl. Phys. A326 (1979) 193
16. T. Suzuki and D.J. Rowe, Nucl. Phys. A289 (1977) 461
 17. A.E.L. Dieperink, Prog. Part. Nucl. Phys. 9(1983) p121.
 18. M. Sambataro, O. Scholten, A.E.L. Dieperink, and G. Piccitto, Nucl. Phys. A423 (1984) 333.
 19. D.R. Bes and R.A. Broglia, Phys. Lett. 137B (1984) 141.
 20. E. Lipparini and S. Stringari, Phys. Lett. 130B (1983) 139.
 21. A. Arima, T. Otsuka, F. Iachello and I. Talmi, Phys. Lett. 66B (1977) 20.
 22. A. Richter, Lecture given a San Miniato, Italy, August 1983, preprint IKDA 83/28.
 23. A. Richter, Private Communication.
 24. H. Sagawa, Invited Paper, Oaxtepec Symposium, Mexico 1984.
 25. O. Scholten, Ph. D. Thesis, Univ. of Groningen 1980.
 26. H. Sagawa, Contributed paper, International Workshop on Interacting Boson-Boson and Boson-Fermion Systems, Gull Lake, Michigan 1984.